AdvART: Adversarial Art for Camouflaged Object Detection Attacks

Amira Guesmi¹, Ioan Marius Bilasco², Muhammad Shafique¹, and Ihsen Alouani³

¹eBrain Laboratory, NYU Abu Dhabi, UAE

²CRIStAL, Univ. Lille, CNRS, Centrale Lille, UMR 9189, France

³CSIT, Queen's University Belfast, UK

Abstract-A majority of existing physical attacks in the real world result in conspicuous and eye-catching patterns for generated patches, which made them identifiable/detectable by humans. To overcome this limitation, recent work has proposed several approaches that aim at generating naturalistic patches using generative adversarial networks (GANs), which may not catch human's attention. However, these approaches are computationally intensive and do not always converge to natural looking patterns. In this paper, we propose a novel lightweight framework that systematically generates naturalistic adversarial patches without using GANs. To illustrate the proposed approach, we generate adversarial art (AdvART), which are patches generated to look like artistic paintings while maintaining high attack efficiency. In fact, we redefine the optimization problem by introducing a new similarity objective. Specifically, we leverage similarity metrics to construct a similarity loss that is added to the optimized objective function. This component guides the patch to follow a predefined artistic patterns while maximizing the victim model's loss function. Our patch achieves high success rates with 12.53% mean average precision (mAP) on YOLOv4tiny

Index Terms—Machine Learning Security, Adversarial Patch, Physical Adversarial Attacks, Object Detectors, Artistic Adversarial Patches

I. Introduction

In the past few years, an increasing number of deep learning (DL) models have been applied to solving a wide range of reallife problems. Deep Neural Networks (DNNs) achieve outstanding performance and flexibility due to their ability to automatically learn features through multiple levels of abstraction. DNN based real-time object detection systems are being increasingly deployed in safetycritical and security-sensitive domains such as video surveillance [1]– [3], self-driving cars [4], health-care [5], etc. However, DNNs suffer from a critical security vulnerability, as related work has demonstrated that these networks are vulnerable to adversarial perturbations [6]–[9]. These malicious examples can even be physically produced in the real world [10]–[13].

The threat model is different between physical attacks and digital attacks. In a digital attack setting [6], [14], an attacker willfully adds adversarial noise to the digital input image, that is optimized to be undetectable by human eyes. The noise undetectability in this case is monitored by the noise budget constraint in the generation process. On the other hand, in a physical attack settings [11]–[13], the attacker designs adversarial patches that are printable in the physical world and deploys it in the scene that is captured by the victim model. These adversarial patches are not generated under noise magnitude constraints but rather under location and printability constraints. Due to its practical application in real-world circumstances, the physical patches based attacks are more practical and damaging for real life scenarios. In this paper, we consider adversarial patches and more precisely investigate the undetectability from naturalistic distribution perspective.

Most of previous works developing adversarial patches for object detection [15]-[17] mainly focus on the attack performance, and



Fig. 1: AdvART generated patches.

enhancing the strength of the adversarial noise. This leads to conspicuous patches which can easily be recognized by human observers. To address this problem, certain works proposed using generative adversarial networks (GANs) [18]–[21]. However, these approaches are very resource consuming and in some cases inefficient as they may not always converge to natural-looking (realistic) patterns. Figure 2 illustrates a few attempts that failed to produce a realistic pattern (refer to Section II for the experimental setup and further information).

In addition, GAN-based techniques are time hungry. In fact, generating a patch can take up to 48 hours. In order to generate fast attacks that are able to generate effective naturalistic patterns, we propose to guide the optimization towards a target natural image, while simultaneously maximizing the victim model's loss. Unlike GANs that take more than a day, our attack needs only 1 hour to perform 4000 iterations and produce a naturalistic patch.

We propose a lightweight framework that generates natural looking and illustrate it with artistic adversarial patches with the aim of jeopardizing detection systems. The approach is based on an optimization process of a new objective function that includes a similarity loss to guide the pattern of the generated noise. This latter does not require a lot of resources like those based on GANs. Figure 1 includes illustrations of the produced adversarial patches.

Contributions – The main contributions of this paper are summarized as follows:

 We show that GAN-based approaches do not always converge to realistic patterns (Section II).

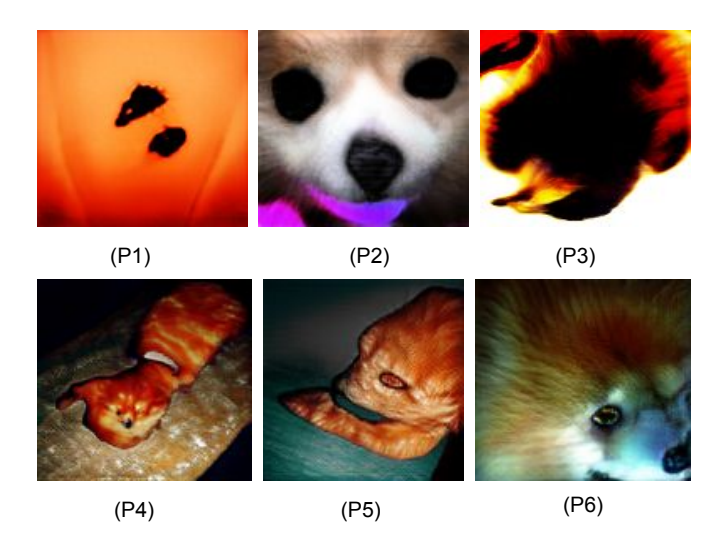


Fig. 2: Failed attempts to generate GAN-based naturalistic patches: (P1) on YOLOv3, (P2) on Faster-CNN, (P3), (P4), (P5), and (P6) on YOLOv2.

- We propose a lightweight framework that generates naturalistic patches that looks like artistic paintings, while retaining attack performance. (Section IV).
- We propose leveraging similarity metrics to force the optimized noise to follow a predefined artistic pattern.
- We thoroughly examine the proposed method's performance in various contexts (Section VI).
- Our patch achieves 12.48% mAP on Yolov4tiny when tested on images from INRIA.

II. MOTIVATION: LIMITATIONS OF GAN-BASED TECHNIQUES

Although GANs are known to be effective in generating images from random noises, they may suffer from some limitations when used to produce naturalistic patches aimed to fool object detectors. In fact, these methods can be time and resource hungry, and in some cases may not converge to realistic patterns. We use the method and code from [20], which provides an approach to generate naturalistic patches based on GANs. We generate patches for the following datasets: CASIA, wildtrack, INRIA, on YOLOv2, YOLOv3, and FasterCNN. Figure 2 illustrates the produced patches using BigGAN generator [22] with an output resolution of 128×128 pretrained on the ImageNet 1k dataset. Same as in [20], we set the class vector to dog. p1 was trained on YOLOv3, p2 on FasterCNN, p3, p4, p5, and p6 on YOLOv2. Patch generation took 24-72 hours depending on the size of the dataset. Generated patches are unrealistic images.

III. RELATED WORK

A. Digital Adversarial Examples

In a digital attack setting, an attacker has the flexibility to arbitrarily alter the input image of a victim model at the pixel level. Thus, these attacks implicitly presuppose that the attacker is in control of the DNN's input system (e.g., a camera). First adversarial example was proposed in [23] which was based on adding small imperceptible noise that tries to push the input image prediction towards the direction of an incorrect class. A number of digital attacks have been proposed advancing the algorithms for producing adversarial examples [6], [14], [24]–[26].

A more robust and realistic threat model would presume that the attacker is exclusively in control of the system's external environment or external objects, rather than its internal sensors and data pipelines. In what follows, we go through some state-of-the-art physical attacks on object detectors.

B. Conspicuous Physical Adversarial Examples

At first, the proposed physical attacks aiming at fooling person detectors were generated without any constraints on the patch appearance. Their main focus was on performance and producing effective attacks. For instance, the work in [16] generates a printable adversarial patch, attached to the person. Able to hide a person from the detector. The produced patch suffers from weak transferability, and the authors did not address issues like robustness to distance/distortions and didn't test detectors beyond Yolov2. Authors in [27] proposed a patch trained for random placement on the scene, causing all existing objects in the image to be missed by the detector. Authors in [28] generated an adversarial T-shirt to hide persons. Authors in [29] proposed an invisibility cloak to fool the detector. All the previously mentioned methods generated patches with conspicuous patterns that could be easily identified.

C. Naturalistic Physical Adversarial Example

To overcome this limitation, some works proposed to leverage the learned image manifold of pre-trained Generative Adversarial Networks (GANs) upon real-world images. Authors in [20] proposed a naturalistic patch based on two GANs (i.e., BigGANN and Style-GAN2). The training on GANs needs a lot of resources in terms of computing units and time to converge if they converge to realistic images in the first place. Authors in [30] also proposed a universal camouflage pattern that is visually similar to natural images. In [18], authors tried to extend the existing work to make the patch suppress objects near the patch. However, what they proposed is unrealistic in terms of the positioning of the patch and its size. Also, another limitation of these approaches is that the patch will be restricted to objects that the GAN was trained to produce, these approaches may not always converge to a natural looking patch.

D. Background Knowledge on Object Detectors

Overfeat [31], a combination of a convolution neural network and a sliding window technique, was the first deep neural network for object detection to be proposed. Regions using Convolutional Neural Networks (R-CNN), employs a search algorithm to provide region proposals and a CNN to name each region. The region proposal algorithm of R-CNN is too slow to be used in real-time, which is a drawback. Later studies, such as, Fast R-CNN [32] and Faster R-CNN [33], substitute a CNN for this inefficient approach. The aforementioned algorithms approach object identification as a twostage problem with proposals for regions and classifications for each of these regions. A single CNN is run over the input image using so-called "single shot detectors" like YOLO [34] (and the followup YOLOv2 [35], YOLOv3 [36], and YOLOv4 [37]) or SSD [38], which jointly produce confidence ratings for object localisation and classification. These networks can thus process images significantly more quickly while maintaining the same accuracy.

IV. PROPOSED APPROACH

A. Problem formulation

In object detection context, given a benign image I, the purpose of the adversarial attack is to jeopardize the object detector and suppress the target objects using the maliciously designed adversarial example

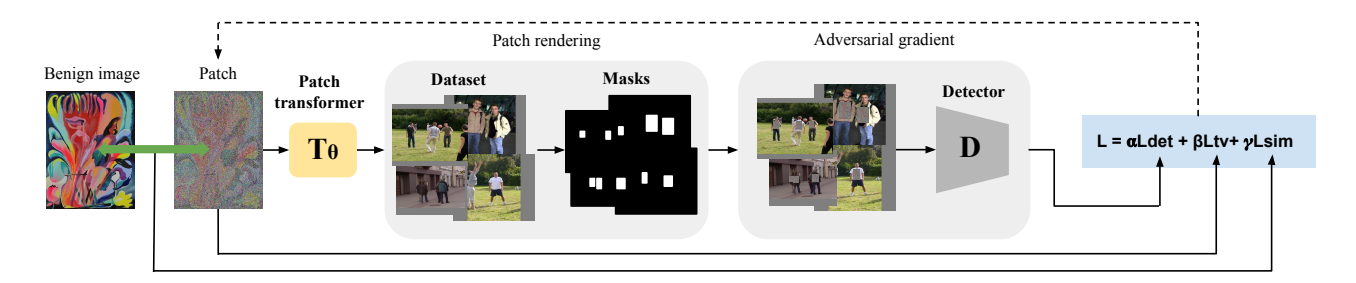


Fig. 3: Overview of the proposed approach: We optimize the adversarial patch P in a way that when placed on a target object, this latter becomes undetectable by an object detector while maintaining the naturalistic and artistic pattern which will be guided by a given benign image. We first feed the patch to the patch transformer to perform the *geometric transformations* in order to make the patch more robust. We, later on, render the patch on top of the input image using the generated masks. After that, we feed the resulting adversarial image to the object detector to compute the detection loss. Then, we compute the gradient of the patch and based on this information we update the patch P.

 I^* . Technically, the adversarial example with generated patch can be formulated as:

$$I^* = (1 - M_P) \odot I + M_P \odot P \tag{1}$$

 \odot is the component-wise multiplication, P is the adversarial patch, and M_P is the patch mask, used to constrict the size, shape, and location of the adversarial patch. The problem of generating an adversarial example can be formulated as a constrained optimization 2, given an original input image I and an object detector F(.):

$$\min_{P} \|P\|_{p} \ s.t.F((1 - M_{P}) \odot I + M_{P} \odot P) \neq F(I)$$
 (2)

The objective is to find a minimal adversarial noise, P, such that when placed on an arbitrary object from a target input domain U, it will selectively jeopardize underlying DNN-based model F(.) by making objects undetectable. Note that one cannot find a closed form solution for this optimization problem since the DNN-based model F(.) is a non-convex machine learning model. Therefore, Equation 2 can be formulated as follows to numerically solve the problem using empirical approximation techniques:

$$\arg\max_{P} \sum_{I \in \mathcal{U}} l(F((1 - M_P) \odot I + M_P \odot P), F(I)$$
 (3)

where l is a predefined loss function and $\mathcal{U} \subset U$ is the attacker's training dataset. We can use existing optimization techniques (e.g., Adam [39]) to solve this problem. In each iteration of the training the optimizer updates the adversarial patch P.

B. Overview

Our goal in this paper is to generate physical adversarial patches that are able to camouflage an object and fool a DNN-based object detector without being conspicuous and attention-grabbing and without using a lot of resources. To achieve this, we propose an objective function that includes a similarity loss which will ensure the artistic pattern of the adversarial patch combined by a detection loss to maintain the performance of the attack while taking into account the complicated physical factors, such as object size, shape, and location.

Figure 3 represents an overview of the proposed framework. We optimize the adversarial patch P in a way that the target object becomes undetectable by an object detector while maintaining the naturalistic and artistic pattern guided by a given benign image. We first feed the patch to the patch transformer and perform the geometric

transformations to make the patch more robust. We, later on, render the patch on top of the input image using the generated masks. After that, we feed the resulting adversarial image to the object detector to compute the detection loss. Then, we compute the gradient of the patch and based on this information we update the patch P.

C. Patch Rendering

In a physical attack scenario, we are unable to manage the adversarial patch's position in relation to the captured scene's objects, its size, or its perspective. Therefore, we render our patch on top of the target object (the human clothing) and simulate various scenes at different settings in order to make it more resilient to a wide variety of possibilities. To simulate how our adversarial patch P could look like in a real-world situation, additional transformations, such as rotation and occlusion, are also incorporated into the optimization process.

D. Patch Transformation

We incorporate the physical world variables throughout the adversarial patch optimization process to successfully deceive DNN-based object detectors in realistic scenarios. Various factors, such as fluctuating lighting, various viewpoints, noise, etc., are frequently present in real-world scenarios. In order to model such dynamic factors, we employ a number of physical changes. Technically speaking, we account for changes caused by the inclusion of various conditions, such as noise addition, random rotation, varying scales, lighting variance, and so forth. The patch transformer creates the physical transformation procedures mentioned above.

The patch was randomly scaled to a size that is nearly proportional to its actual size in the scene as part of the geometric changes. Rotate the patch P at random $(\pm 20^\circ)$ about the center of the bounding boxes. The aforementioned replicates printing size and location inaccuracies. The pixel intensity values are altered by adding random noise $((\pm 0.1)$, conducting random contrast adjustment of the value ([0.8, 1.2]), and doing random brightness adjustment (± 0.1) to create the color space conversions. The resulting image $T_{\theta}(I_i)$ is forward propagated through the detector.

E. Attack Scenario

Our goal is to generate physical adversarial patches that are natural looking while still maintaining their attack performance. We iteratively perform gradient updates on the adversarial patch (P) in the pixel space that optimizes our objective defined as follows:

$$Loss_{total} = \alpha L_{det} + \beta L_{sim} + \gamma L_{tv} \tag{4}$$

Where L_{det} is the adversarial detection loss. L_{sim} is the similarity loss

 L_{tv} is the total variation loss on the generated image to encourage smoothness. It is defined as:

$$L_{tv} = \sum_{i,j} \sqrt{(P_{i+1,j} - P_{i,j})^2 + (P_{i,j+1} - P_{i,j})^2}$$
 (5)

where the subindices i and j refer to the pixel coordinate of the patch P.

 α , β , and γ are hyper-parameters used to scale the three losses. For our experiments we set $\alpha=2$, $\beta=0.5$, and $\gamma=1.5$ We optimize the total loss using Adam [39] optimizer. We try to minimize the object function L_{total} and optimize the adversarial patch. We freeze all weights and biases in the object detector, and only update the pixel values of the adversarial patch. The patch is randomly initialized.

F. Adversarial Detection Loss

Object detectors, such as YOLO, output an arbitrary number of boxes or detections. For each detection j, we are interested in attacking two quantities: its objectness probability D^j_{obj} and its class probability D^j_{olj} . Minimizing the objectness probability D^j_{obj} causes the j-th object not to get detected. Minimizing class probability D^j_{olj} causes the j-th object to get classified into the wrong class (e.g. person gets classified as a dog.). In this paper, we focus on targeting the person class. Thus, we minimized both the objectness D^j_{obj} and class probabilities D^j_{cls} pertaining to the person class. For faster iterations, we do not compute the loss over all detected boxes. Instead, we only use the detected box having the highest objectness and class probabilities. Our adversarial detection loss is defined below:

$$L_{det} = \frac{1}{N} \sum_{i=1}^{N} max_{j} [D_{obj}^{j}(I_{i}') D_{cls}^{j}(I_{i}')]$$
 (6)

G. Adversarial Similarity Loss

 L_{sim} is the similarity loss between the target natural image N and the adversarial patch P. It is defined as:

$$L_{sim} = \left(\frac{1}{N} \sum_{i,j} (|P_{i,j} - N_{i,j}|)\right)^2 \tag{7}$$

We square the difference between the benign image and the adversarial patch, as in quadratic functions the rate of increase (the slope or the rate of change) is slower which delays the convergence of the similarity metric with respect to the detection loss. In fact, the similarity metric is a linear function compared to the detection metric which is a non-linear function that converges much slower.

V. EXPERIMENTAL SETUP

As victim object detectors, we used Yolov2 [35] YOLOv3 [36], YOLOv3tiny, YOLOv4 [37], and YOLOv4tiny with an input image resolution of 416×416 . For the optimization, we use Adam optimizer with a learning rate of 0.005, $\beta 1 = 0.9$ and $\beta 2 = 0.999$.

In our evaluations, we use the images of the Inria [40] and the MPII [41] datasets. **INRIA person dataset** is intended for pedestrians which makes it suitable for our proposed setting. The dataset is popular in the Pedestrian Detection community, both for training detectors and reporting results. It consists of 614 person detections for training and 288 for testing. **MPII Human Pose dataset** is a state of the art benchmark for evaluation of articulated human pose estimation. The dataset includes around 25K images containing over

 $40 \mathrm{K}$ people with annotated body joints. Same as in [20], We also performed cross-dataset evaluations using the MPII Human Pose dataset to test the generalization of the proposed approach. We selected pictures in categories "running", "walking", and "dancing" classes. This results in a total of 1,646 images, which we split into 1,317 training and 329 testing images. Similarly, all the images are scaled to 416×416 .

VI. EVALUATION OF ATTACK PERFORMANCE

We use the mean average precision (mAP) as our evaluation metric. Same as in [16], [20], we utilize each detector's detection boxes on the clean dataset as the ground truth boxes (i.e., if there is no adversarial patch, the mAP of detectors will be 100%) and we report the mean average precision (mAP) when adding the adversarial patches. Table I shows the evaluation results on the INRIA dataset. We utilize five different detectors to train the patches. The horizontal detectors are the victim ones and the verticals are the ones used for training.

As shown in Table I, when the victim detector used for training is the same used for testing, we accomplish a very good attack performance. Additionally, our technique can also do well against detectors that were not used for training which proves the transferability across models of our attack.



Fig. 4: AdvART patch vs State-of-the-Art patches: (a) AdvART patch, (b) Naturalistic patch [20], (c) Adversarial patch [16], and (d) UPC patch [30].

A. Cross-Dataset Evaluation

We use Yolov4tiny to train an adeversarial patch on the INRIA dataset and test the produced patch on the MPII dataset. As shown in Table II, our patch is transferable cross-datasets. In fact, an adversarial patch generated on the INRIA dataset is still effective on MPII. For instance, a patch generated for the INRIA dataset with a mAP equal to 12.48% has a mPA equal to 15.53% on MPII dataset.

B. AdvART vs State-of-the-Art Techniques

We compare the performance of our patch against state of the art adversarial patches: Naturalistic patches, Adversarial patches, and Universal physical camouflage proposed in [20], [16], and [30], respectively. Mean average precision results are reported in

TABLE I: Attack performance (mAP) of AdvART on INRIA dataset using different detectors.

| Models | YOLOv2 | YOLOv3 | YOLOv3tiny | YOLOv4 | YOLOv4tiny |
|-----------------|--------|---------|------------|---------|------------|
| (P1) YOLOv2 | 20.8% | 35.67% | 37.61% | 36.20% | 65.43% |
| (P2) YOLOv3 | - | 15.82% | 52.77% | 29.37% | 58.24% |
| (P3) YOLOv3tiny | - | 41.46% | 34.93% | 37.46% | 56.29% |
| (P4) YOLOv4 | - | 27.18 % | 41.36% | 17.7% | 65.84% |
| (P5) YOLOv4tiny | - | 60.70% | 57.40% | 47.46 % | 12.48% |

TABLE II: Attack performance (mAP) of AdvART on MPII.

| Datasets | mAP | |
|----------|---------|--|
| INRIA | 12.48% | |
| MPII | 15.53 % | |

Table III. Although Adversarial Patches [16] delivers the best attack performance, the patches it generates lack realism and are very eyecatching. On the other hand, while maintaining acceptable attack performance, our suggested method can produce adversarial patches that look very natural. Our patch delivers comparable performance to that of state of the art techniques, while having realistic artistic patterns.

VII. DISCUSSION

A. Influence of Patch Size

We run a number of digital experiments on the INRIA dataset to assess the performance influence of the patch size with respect to the size of the target object (person). Table IV shows that the larger the size of the patch is, the stronger its attack performance as expected.

B. Patch robustness against Input Transformation-based Defenses

We use three commonly used defense approaches that perform input transformations without re-training the victim models to assess the robustness of our patch against these defenses. We use JPEG compression [42], add Gaussian noise [43], Median blurring [44]. We report the mean average precision of the benign scenarios, i.e., when applying the defense technique on the benign images and of the adversarial scenario, i.e., when applying the defense on the adversarial image. We notice that our patch is still effective even when using defense techniques (See Tables V, VI, and VII).

VIII. CONCLUSION

In this paper, we introduce a novel approach for producing realistic physical adversarial patches for object detectors. AdvART is a lightweight framework that does not require a lot of computations as compared to GAN-based approaches, and it is capable of successfully producing realistic adversarial patches with artistic patterns while retaining competitive attack performance compared to GAN-based techniques and non-naturalistic ones. Our approach is more than 24 times faster than GAN-based techniques, delivering naturalistic and artistic patches.

REFERENCES

- [1] K. Boudjit and N. Ramzan, "Human detection based on deep learning yolo-v2 for real-time uav applications," *Journal of Experimental & Theoretical Artificial Intelligence*, vol. 34, no. 3, pp. 527–544, 2022.
- [2] A. Sabater, L. Montesano, and A. C. Murillo, "Robust and efficient post-processing for video object detection," in 2020 IEEE/RSJ International Conference on Intelligent Robots and Systems (IROS). IEEE, 2020, pp. 10536–10542.
- [3] A. Mangawati, Mohana, M. Leesan, and H. V. R. Aradhya, "Object tracking algorithms for video surveillance applications," in 2018 International Conference on Communication and Signal Processing (ICCSP), 2018, pp. 0667–0671.

- [4] M. Al-Qizwini, I. Barjasteh, H. Al-Qassab, and H. Radha, "Deep learning algorithm for autonomous driving using googlenet," in 2017 IEEE Intelligent Vehicles Symposium (IV). IEEE, 2017, pp. 89–96.
- [5] R. Miotto, F. Wang, S. Wang, X. Jiang, and J. T. Dudley, "Deep learning for healthcare: review, opportunities and challenges," *Briefings* in bioinformatics, vol. 19, no. 6, pp. 1236–1246, 2018.
- [6] N. Carlini and D. A. Wagner, "Towards evaluating the robustness of neural networks," *CoRR*, vol. abs/1608.04644, 2016. [Online]. Available: http://arxiv.org/abs/1608.04644
- [7] B. Li and Y. Vorobeychik, "Scalable optimization of randomized operational decisions in adversarial classification settings," in Proceedings of the Eighteenth International Conference on Artificial Intelligence and Statistics, AISTATS 2015, San Diego, California, USA, May 9-12, 2015, ser. JMLR Workshop and Conference Proceedings, G. Lebanon and S. V. N. Vishwanathan, Eds., vol. 38. JMLR.org, 2015. [Online]. Available: http://proceedings.mlr.press/v38/li15a.html
- [8] A. M. Nguyen, J. Yosinski, and J. Clune, "Deep neural networks are easily fooled: High confidence predictions for unrecognizable images," *CoRR*, vol. abs/1412.1897, 2014. [Online]. Available: http://arxiv.org/abs/1412.1897
- [9] N. Papernot, P. D. McDaniel, S. Jha, M. Fredrikson, Z. B. Celik, and A. Swami, "The limitations of deep learning in adversarial settings," *CoRR*, vol. abs/1511.07528, 2015. [Online]. Available: http://arxiv.org/abs/1511.07528
- [10] I. Evtimov, K. Eykholt, E. Fernandes, T. Kohno, B. Li, A. Prakash, A. Rahmati, and D. Song, "Robust physical-world attacks on machine learning models," *CoRR*, vol. abs/1707.08945, 2017. [Online]. Available: http://arxiv.org/abs/1707.08945
- [11] A. Kurakin, I. J. Goodfellow, and S. Bengio, "Adversarial examples in the physical world," *CoRR*, vol. abs/1607.02533, 2016. [Online]. Available: http://arxiv.org/abs/1607.02533
- [12] I. Evtimov, K. Eykholt, E. Fernandes, T. Kohno, B. Li, A. Prakash, A. Rahmati, and D. Song, "Robust physical-world attacks on machine learning models," *CoRR*, vol. abs/1707.08945, 2017. [Online]. Available: http://arxiv.org/abs/1707.08945
- [13] V. Venceslai, A. Marchisio, I. Alouani, M. Martina, and M. Shafique, "Neuroattack: Undermining spiking neural networks security through externally triggered bit-flips," 2020.
- [14] I. J. Goodfellow, J. Shlens, and C. Szegedy, "Explaining and harnessing adversarial examples," 2015.
- [15] K. Eykholt, I. Evtimov, E. Fernandes, B. Li, A. Rahmati, F. Tramèr, A. Prakash, T. Kohno, and D. Song, "Physical adversarial examples for object detectors," in *Proceedings of the 12th USENIX Conference on Offensive Technologies*, ser. WOOT'18. USA: USENIX Association, 2018, p. 1.
- [16] S. Thys, W. V. Ranst, and T. Goedemé, "Fooling automated surveillance cameras: adversarial patches to attack person detection," *CoRR*, vol. abs/1904.08653, 2019. [Online]. Available: http://arxiv.org/abs/1904. 08653
- [17] Y. Zhao, H. Zhu, R. Liang, Q. Shen, S. Zhang, and K. Chen, "Seeing isn't believing: Towards more robust adversarial attack against real world object detectors," ser. CCS '19. New York, NY, USA: Association for Computing Machinery, 2019, p. 1989–2004. [Online]. Available: https://doi.org/10.1145/3319535.3354259
- [18] S. Pavlitskaya, B.-M. Codău, and J. M. Zöllner, "Feasibility of inconspicuous gan-generated adversarial patches against object detection," 2022. [Online]. Available: https://arxiv.org/abs/2207.07347
- [19] T. Bai, J. Luo, and J. Zhao, "Inconspicuous adversarial patches for fooling image-recognition systems on mobile devices," *IEEE Internet* of Things Journal, vol. 9, no. 12, pp. 9515–9524, 2022.
- [20] Y.-C.-T. Hu, J.-C. Chen, B.-H. Kung, K.-L. Hua, and D. S. Tan, "Naturalistic physical adversarial patch for object detectors," in 2021

TABLE III: AdvART vs state-of-the-art adversarial patches.

| Models | AdvART patches | Naturalistic patches [20] | Adversarial patches [16] | UPC [30] |
|------------|----------------|---------------------------|--------------------------|----------|
| YOLOv2 | 20.8% | 12.06% | 2.13% | 48.62% |
| YOLOv3 | 15.82% | 34.93 % | 22.51% | 54.40% |
| YOLOv3tiny | 34.93% | 10.02% | 8.74% | 63.82% |
| YOLOv4 | 17.7 % | 22.63% | 12.89% | 64.21 % |
| YOLOv4tiny | 12.48% | 8.67% | 3.25% | 57.93 % |

TABLE IV: Attack performance of adversarial patches in different size settings for the INRIA dataset.

| Patch size | mAP |
|------------|--------|
| 0.1 | 55.7% |
| 0.2 | 12.48% |
| 0.3 | 6.32% |

TABLE V: Attack performance of adversarial patch when using JPEG Compression defense in a benign and adversarial scenario.

| Parameters | Benign Scenario | Adversarial Scenario |
|------------|-----------------|----------------------|
| 90 | 98.03% | 25.34% |
| 70 | 95.3% | 31.98% |
| 50 | 90.23% | 42% |
| 30 | 80.1% | 50.5% |

TABLE VI: Attack performance of adversarial patch when using Gaussian Noise defense in a benign and adversarial scenario.

| Parameters | Benign Scenario | Adversarial Scenario |
|------------|-----------------|----------------------|
| 0.01 | 80% | 45.3% |
| 0.02 | 75.1% | 47.43% |
| 0.05 | 78.65% | 50.2% |
| 0.1 | 70.44% | 55.23% |

TABLE VII: Attack performance of adversarial patch when using Median Blurring defense in a benign and adversarial scenario.

| Parameters | Benign Scenario | Adversarial Scenario |
|------------|-----------------|----------------------|
| 5 | 99.3% | 22.34% |
| 10 | 96.76% | 21.12% |
| 15 | 93.44% | 42.2% |
| 20 | 87.30% | 30.11% |

IEEE/CVF International Conference on Computer Vision (ICCV), 2021, pp. 7828–7837.

- [21] J. Liu, Y. Tian, R. Zhang, Y. Sun, and C. Wang, "A two-stage generative adversarial networks with semantic content constraints for adversarial example generation," *IEEE Access*, vol. 8, pp. 205766–205777, 2020.
- [22] A. Voynov and A. Babenko, "Unsupervised discovery of interpretable directions in the gan latent space," in *International Conference on Machine Learning*. PMLR, 2020, pp. 9786–9796.
- [23] C. Szegedy, W. Zaremba, I. Sutskever, J. Bruna, D. Erhan, I. J. Goodfellow, and R. Fergus, "Intriguing properties of neural networks," in 2nd International Conference on Learning Representations, ICLR 2014, Banff, AB, Canada, April 14-16, 2014, Conference Track Proceedings, Y. Bengio and Y. LeCun, Eds., 2014. [Online]. Available: http://arxiv.org/abs/1312.6199
- [24] W. Brendel, J. Rauber, and M. Bethge, "Decision-based adversarial attacks: Reliable attacks against black-box machine learning models," 2017
- [25] N. Narodytska and S. P. Kasiviswanathan, "Simple black-box adversarial perturbations for deep networks," *CoRR*, vol. abs/1612.06299, 2016. [Online]. Available: http://arxiv.org/abs/1612.06299
- [26] J. Chen and M. I. Jordan, "Boundary attack++: Query-efficient decision-based adversarial attack," CoRR, vol. abs/1904.02144, 2019.

- [Online]. Available: http://arxiv.org/abs/1904.02144
- [27] M. Lee and J. Z. Kolter, "On physical adversarial patches for object detection," CoRR, vol. abs/1906.11897, 2019. [Online]. Available: http://arxiv.org/abs/1906.11897
- [28] K. Xu, G. Zhang, S. Liu, Q. Fan, M. Sun, H. Chen, P.-Y. Chen, Y. Wang, and X. Lin, "Adversarial t-shirt! evading person detectors in a physical world," in ECCV, 2020.
- [29] Z. Wu, S.-N. Lim, L. S. Davis, and T. Goldstein, "Making an invisibility cloak: Real world adversarial attacks on object detectors," in ECCV, 2020.
- [30] L. Huang, C. Gao, Y. Zhou, C. Zou, C. Xie, A. L. Yuille, and N. Liu, "UPC: learning universal physical camouflage attacks on object detectors," *CoRR*, vol. abs/1909.04326, 2019. [Online]. Available: http://arxiv.org/abs/1909.04326
- [31] P. Sermanet, D. Eigen, X. Zhang, M. Mathieu, R. Fergus, and Y. LeCun, "Overfeat: Integrated recognition, localization and detection using convolutional networks," 2014, publisher Copyright: © 2014 International Conference on Learning Representations, ICLR. All rights reserved.; 2nd International Conference on Learning Representations, ICLR 2014 ; Conference date: 14-04-2014 Through 16-04-2014.
- [32] R. B. Girshick, "Fast R-CNN," CoRR, vol. abs/1504.08083, 2015.
 [Online]. Available: http://arxiv.org/abs/1504.08083
- [33] S. Ren, K. He, R. B. Girshick, and J. Sun, "Faster R-CNN: towards real-time object detection with region proposal networks," *CoRR*, vol. abs/1506.01497, 2015. [Online]. Available: http://arxiv.org/abs/1506. 01497
- [34] J. Redmon, S. K. Divvala, R. B. Girshick, and A. Farhadi, "You only look once: Unified, real-time object detection," *CoRR*, vol. abs/1506.02640, 2015. [Online]. Available: http://arxiv.org/abs/1506.02640
- [35] J. Redmon and A. Farhadi, "YOLO9000: better, faster, stronger," CoRR, vol. abs/1612.08242, 2016. [Online]. Available: http://arxiv.org/abs/1612.08242
- [36] —, "Yolov3: An incremental improvement," arXiv, 2018.
- [37] H.-Y. M. L. Alexey Bochkovskiy, Chien-Yao Wang, "Yolov4: Yolov4: Optimal speed and accuracy of object detection," arXiv, 2020.
- [38] W. Liu, D. Anguelov, D. Erhan, C. Szegedy, S. E. Reed, C. Fu, and A. C. Berg, "SSD: single shot multibox detector," *CoRR*, vol. abs/1512.02325, 2015. [Online]. Available: http://arxiv.org/abs/1512.02325
- [39] D. P. Kingma and J. Ba, "Adam: A method for stochastic optimization," 2014. [Online]. Available: https://arxiv.org/abs/1412.6980
- [40] N. Dalal and B. Triggs, "Histograms of oriented gradients for human detection," in 2005 IEEE Computer Society Conference on Computer Vision and Pattern Recognition (CVPR'05), vol. 1, 2005, pp. 886–893 vol. 1.
- [41] M. Andriluka, L. Pishchulin, P. Gehler, and B. Schiele, "2d human pose estimation: New benchmark and state of the art analysis," in *IEEE Conference on Computer Vision and Pattern Recognition (CVPR)*, June 2014.
- [42] G. K. Dziugaite, Z. Ghahramani, and D. M. Roy, "A study of the effect of JPG compression on adversarial images," *CoRR*, vol. abs/1608.00853, 2016. [Online]. Available: http://arxiv.org/abs/1608.00853
- [43] Y. Zhang and P. Liang, "Defending against whitebox adversarial attacks via randomized discretization," in *Proceedings of the Twenty-Second International Conference on Artificial Intelligence and Statistics*, ser. Proceedings of Machine Learning Research, K. Chaudhuri and M. Sugiyama, Eds., vol. 89. PMLR, 16–18 Apr 2019, pp. 684–693. [Online]. Available: https://proceedings.mlr.press/v89/zhang19b.html
- [44] W. Xu, D. Evans, and Y. Qi, "Feature squeezing: Detecting adversarial examples in deep neural networks," *CoRR*, vol. abs/1704.01155, 2017. [Online]. Available: http://arxiv.org/abs/1704.01155